EAN 2020
58th conference on experimental stress analysis

On Cyclic Hardening/Softening Behaviour of Conventional and 3D Printed SS316L

HALAMA R.[1,a], GÁL P.[1,b], PAGÁČ M.[1,c], GOVINDARAJ B.[1,d]
KOCICH R.[2,e], KUNČICKÁ L.[2,f]

[1]Faculty of Mechanical Engineering, VŠB – Technical University of Ostrava, 17. listopadu 2172/15, 708 00 Ostrava, Czech Republic

[2]Faculty of Materials Science and Technology, VŠB – Technical University of Ostrava, 17. listopadu 2172/15, 708 00 Ostrava, Czech Republic

[a]radim.halama@vsb.cz, [b]petr.gal.st@vsb.cz, [c]marek.pagac@vsb.cz, [d]bhuvanesh.govindaraj.st@vsb.cz, [e]radim.kocich@vsb.cz, [f]lenka.kuncicka@vsb.cz

Keywords: non-proportional hardening, SS316L, additive manufacturing, low cycle fatigue

Abstract.
This study is focused mainly on the stress-strain behaviour investigation under proportional as well as non-proportional loading on SS316L made by casting and prepared by Selective Laser Melting. Strain controlled fatigue tests have been performed under constant strain amplitude loading considering a constant strain rate. Influence of non-proportionality degree on the additional cyclic hardening is also investigated showing that the square loading path lead to the maximal level of non-proportional hardening. Both variants of SS316L are compared from the mechanical as well as microstructural point of view.

Introduction

The increasing demands on modern materials go hand in hand with the requirement to develop innovative alloys to widen the possibilities of application of metallic materials, as well as to enhance the utility properties and increase the longevity of products manufactured based on the known material systems. Among the favourable ways how to enhance the properties of metallic materials is to alter their structure, preferably having in mind the Hall-Petch relation [1] which stating that decreasing the grain size within the structure introduces increased mechanical properties, especially strength. Various non-conventional methods the grain size by which can be decreased have been introduced, such as the severe plastic deformation (SPD) technologies [2-5]. Nevertheless, the absolute values of the average grain size after processing also depends on the initial grain size of the original material. By this reason, fabrication of modern materials from initial powders has gained a lot of attention recently [6].

Selective Laser Melting (SLM) belongs to the group of additive manufacturing, or rapid prototyping, technologies using powders to build solid bulk materials [7]. Among its main advantages is the rapid cooling rate (as high as 10^6 K/s), which introduces the possibility to manufacture complex fine-grained structure geometries having microstructures composed of a wide range of crystallographic phases in a relatively easy manner. SLM has successfully been used to produce various materials, from Al-based alloys and composites [8], through Ti-based [9] and Zr-based [10] alloys and high entropy alloy [11], to steels [12].

This work is a continuation of the contribution presented at the ASME PVP2019 conference in Texas [13], where the ratcheting behaviour of 3D printed and conventionally prepared 316L Stainless Steel was presented, including the effects of the applied strain rate on both the

materials. Complex microstructures, as the one presented, lead to a higher yield limit [14,15] of the SS316L material, resulting in higher resistance in load-controlled fatigue tests [13]. The SLM technology shows a significant anisotropic behaviour, studied on SS316L for instance in [16]. The high cycle fatigue behaviour of the material under investigation were reported e.g. by Blinn et al. in ref. [17]. The stress-strain behaviour research presented in [13] shows similar softening behaviour during ratcheting tests and uniaxial low-cycle tests as observed on the Ti-6A-4V [18]. The conventional stainless steel has been investigated in special loading modes. There are published works showing the influence of strain rate on the behaviour of the material under room temperature [19,20].

This study is focused on the comparison of stress-strain behaviours of the 316L steel prepared via conventional casting and SLM technology, with the main focus on strain control in fatigue testing. The 3D printing process used for preparation of the herein presented specimens was identical to the process reported in the previous study [13]. Cyclic hardening/softening material behaviour has been evaluated for proportional, as well as non-proportional loading cases. Results of the technique using DIC for cyclic stress-strain curve estimation from a single low-cycle fatigue test are presented too.

Uniaxial fatigue tests

All tests in this study have been realised under constant strain amplitude and zero mean strain on the LabControl 100kN/1000Nm hydraulic testing machine in VSB-Technical University of Ostrava. Tension-compression fatigue tests were performed using a solid specimen with a diameter of 5mm. The comparison of standard cyclic stress-strain curve for uniaxial loading for additively and conventionally produced SS316L is shown in Fig. 1a. The curves and lifetimes are very similar for both production technologies, see Fig. 1b.

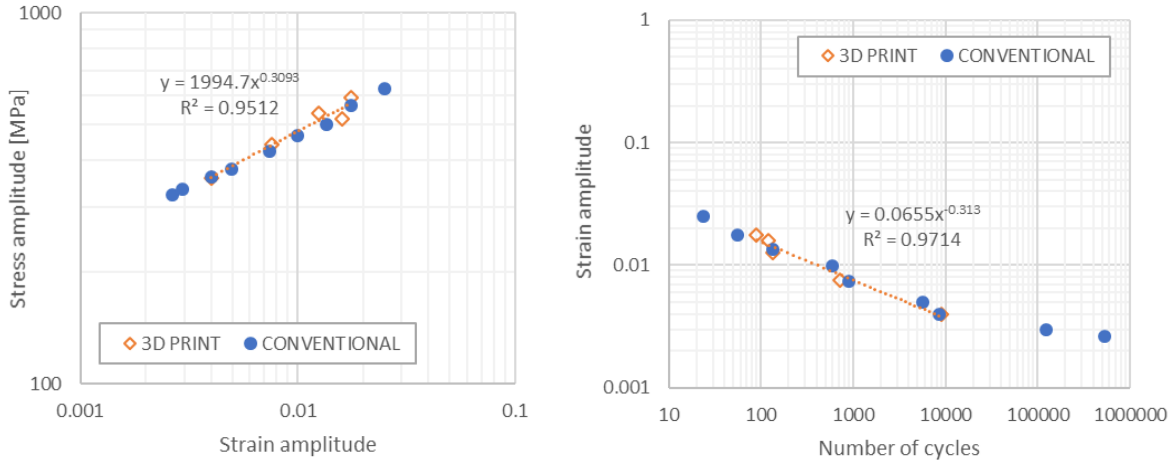

a) b)

Fig. 1: Comparison of uniaxial fatigue test results on conventional and 3D printed SS316L: a) Cyclic stress-strain curves; b) E-N curves

Multiaxial fatigue tests

Multiaxial fatigue testing has been done on a thin-walled specimen with an inner diameter of 10mm and an outer diameter of 12.5 mm [14]. The EPSILON 3550 biaxial extensometer was used to control shear and axial strain (25 mm gauge length) in that case. First, Low-Cycle Fatigue (LCF) tests for different non-proportional load paths and different levels of loading were realised on the conventional SS316L. This steel has low stacking fault energy (SFE) [23] which is sensitive to the additional hardening dependent on the type of material and also on loading path.

First, the stress-strain behaviour of conventional SS316L will be described. The influence of strain paths on transient behaviour during the first several load cycles has been evaluated. In the case of a rhombic path, see Fig. 2a, it is obvious that there is characteristic cyclic hardening following by softening till fracture for a higher level of loading (solid curve). In case of lower loading levels cyclic hardening is followed by the almost steady state after several cycles. In Fig. 2b the axial hysteresis loops are shown for rhombic loading path under 1% of strain amplitude. From this picture is obvious the strong non-proportional hardening during the first several cycles followed by cyclic softening.

A significant change in the shape of the hysteresis loop between the first and tenth cycle is evident from Fig. 2b. A small change on shape is visible between the tenth and twentieth cycle. Other interesting results are reported in [21].

In the case of circle path, see Fig. 3, it is obvious that cyclic hardening, during the first several cycles, is followed almost by the steady state (Fig. 4a). This is in contrast with 3D printed SS316L, where the cyclic softening begins immediately and occurs during the whole test. An interesting observation is that the hysteresis loops in the half-life are very similar in shape and size, see Fig. 4b.

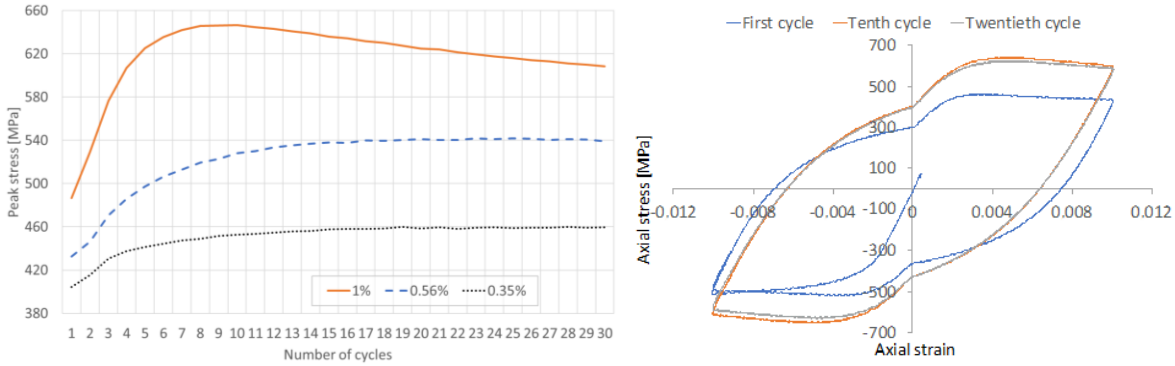

a) b)

Fig. 2: Results of additional hardening due to non-proportional loading: a) Cyclic hardening for rhombic path - conventional SS316L; b) Axial hysteresis loops for the rhombic path under strain amplitude of 1%

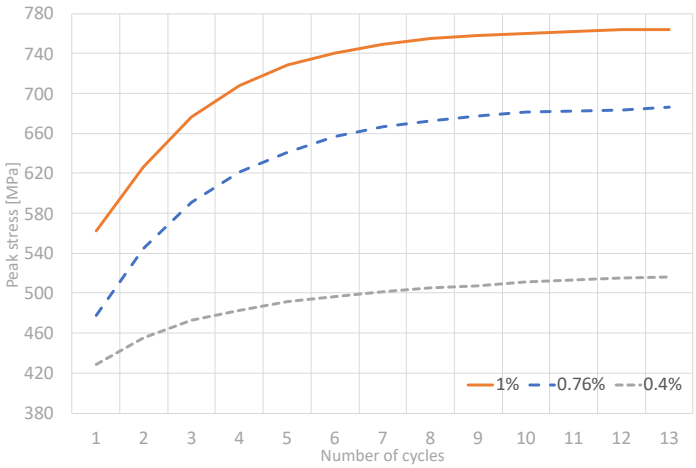

Fig. 3: Results of additional hardening due to non-proportional loading for circle path - conventional SS316L

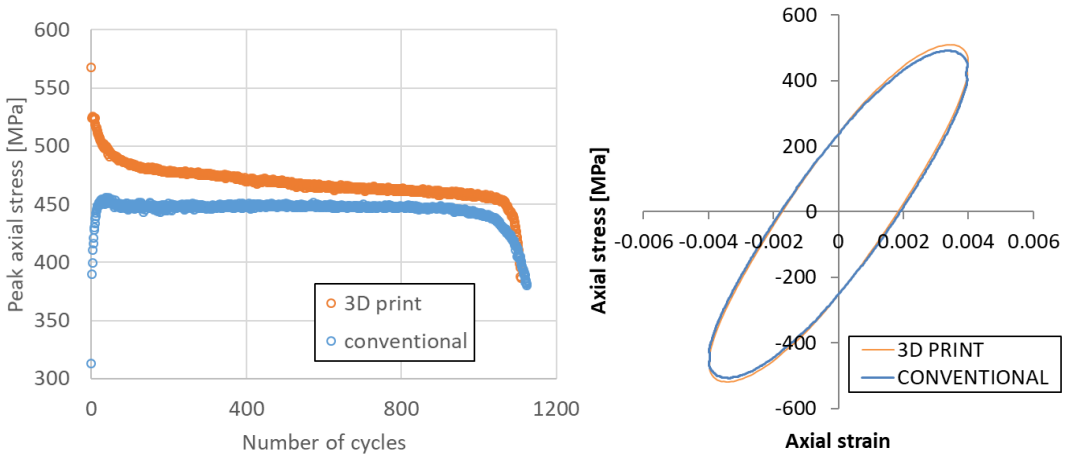

Fig. 4: Experimental results for both variants of SS316L: a) Cyclic hardening-softening curves in 0.4% strain amplitude test with circle path b) Axial hysteresis loops in the half-life

The biggest influence on additional hardening during the first several cycles has the square loading path. Lower influence on non-proportional hardening has the circle and rhombic loading paths. This is evident from Fig. 5, where the experimental results from non-proportional experiments are compared with proportional experimental results (tension/compression tests). Square loading path reveals almost two times bigger stress amplitude than proportional loading path, when comparing higher strain amplitudes. In the case of smaller amplitudes, the differences are quite smaller.

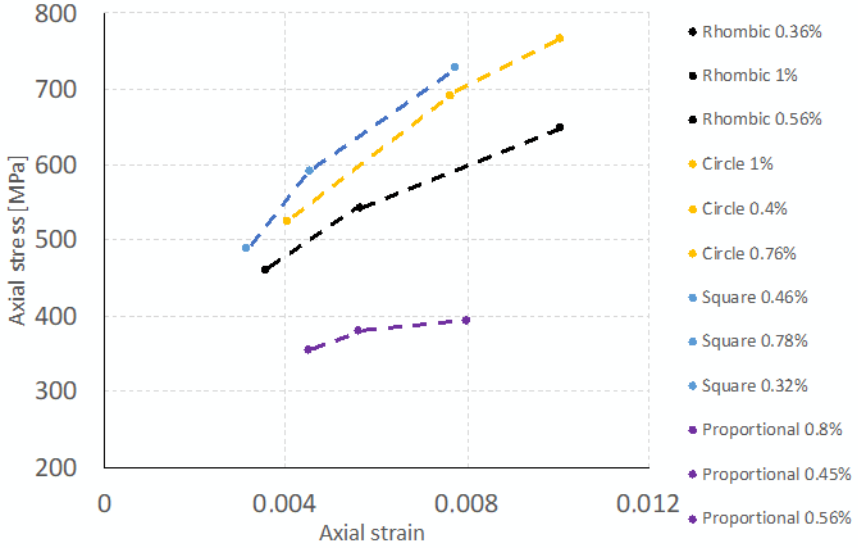

Fig. 5: Peak axial stress vs peak axial strain for different loading paths and strain amplitudes

In cyclic plasticity is the additional hardening usually described by the non-proportional parameter Φ (or different designation). This parameter is usually used at construction of cyclic plasticity or life-time models, like [22]. Some inspiration could be found in [23], where the authors suggest the non-proportional parameter, where they incorporate the additional strain hardening parameter in this form

$$\alpha = \frac{\sigma^n - \sigma^p}{\sigma^p} = \frac{\sigma^n}{\sigma^p} - 1. \qquad (1)$$

The quantities σ^p and σ^n are the basic maximum values of von Mises equivalent stresses under cyclic proportional (tension, compression or torsion) and non-proportional loading paths

deformation, respectively. Using equation (1) the value of non-proportionality for different loading paths and levels of loading can be determined as stated in Tab.1.

Tab. 1 Additional hardening for different loading paths

Path	**Square 0.32 %**	**Square 0.46 %**	**Square 0.78 %**
σ_a [MPa]	525.4	618.9	749.8
α [-]	55.36 %	65.77 %	73.82 %
Path	**Circle 0.4 %**	**Circle 0.76 %**	**Circle 1 %**
σ_a [MPa]	527.2	702.4	753.2
α [-]	45.78 %	63.47 %	62.79 %
Path	**Rhombic 0.36 %**	**Rhombic 0.56 %**	**Rhombic 1 %**
σ_a [MPa]	477.7	574.4	661.3
α [-]	36.61 %	45.12 %	42.88 %

As apparent from Tab. 1, the highest level of additional hardening evokes the Square paths under 0.78 % of strain amplitude of loading. The additional hardening observed is almost 74%. On the other side, the Rhombic loading path is present, which evokes the hardening of 37% under 0.36 % of strain amplitude of loading. It is evident that additional hardening depends not only on the strain path but also on the level of loading. The higher amplitude of loading the more significant non-proportional hardening. The results are consistent with imagination, that under high load level more grains are affected by plastic deformation.

Evaluation of cyclic stress-strain curve by Digital Image Correlation

Digital Image Correlation (DIC) measurement has been done on 3D printed uniaxial specimens to verify the accelerated experimental technique published in [24]. The DIC technique was applied to get the cyclic stress-strain curve of conventional SS316L material from a single low-cycle fatigue test. A detailed description of the experiment and its evaluation is reported elsewhere [25].

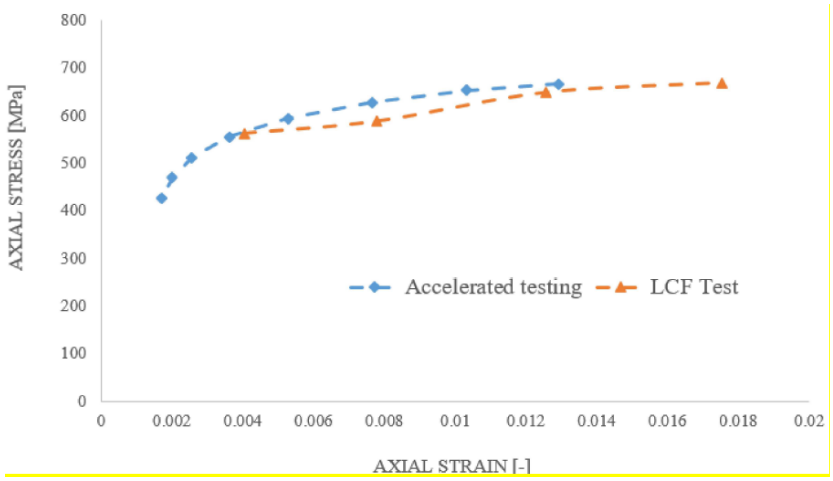

Fig. 6: Peak axial stress vs peak axial strain for different loading paths and strain amplitudes

Structure observations

Analyses of phase composition of both the materials were performed using Scanning Electron Microscopy (SEM-EDX), see Fig. 7. The results of the phase composition analyses of the examined samples show that both the cast and powder structures consisted mostly of austenite. Ferrite occurred mainly in the cast structure, however, only locally, primarily at the boundaries of austenitic grains.

Fig. 8 shows SEM-BSE (back-scattered electrons) images of both the examined materials the low angle (misorientation angle lower than 15°) and high angle (misorientation angle greater than 15°) boundaries (LAGBs and HAGBs) in which are highlighted in red (<15°) and black (> 15°) colours, respectively. Analysis of the grain boundary misorientations showed a fully recovered structure in the cast sample, as the structure exhibited the majority of HAGBs and a negligible presence of LAGBs. This sample also showed the presence of twins.

In contrast, the sample of the material originally printed from powders exhibited a more significant presence of LAGBS, indicating that the grains were not fully recovered and pointing to substructure development. Nevertheless, the content of HAGBs was still prevailing for this sample.

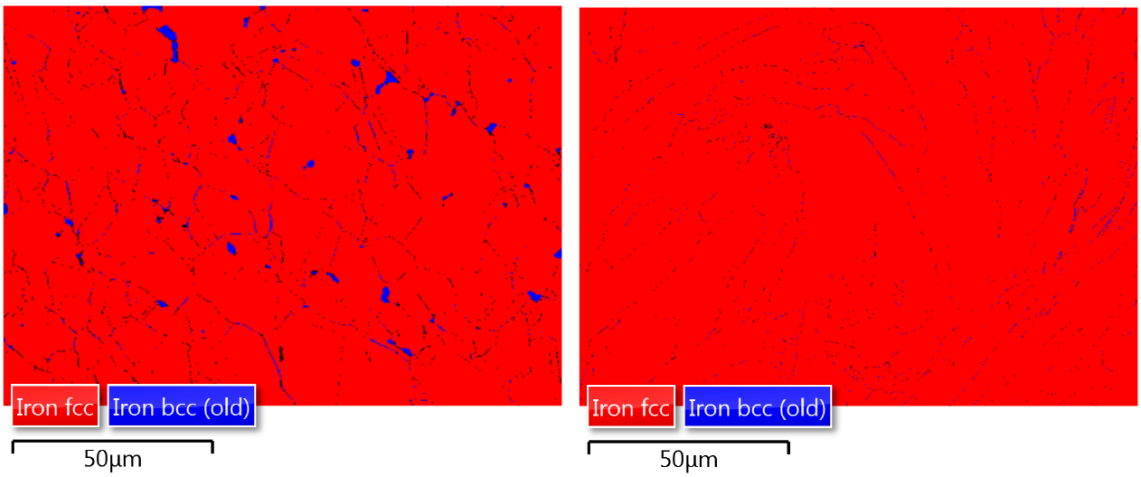

a) b)

Fig. 7: Results of phase composition analysis for both variants of SS316L: a) cast structure b) powder structure

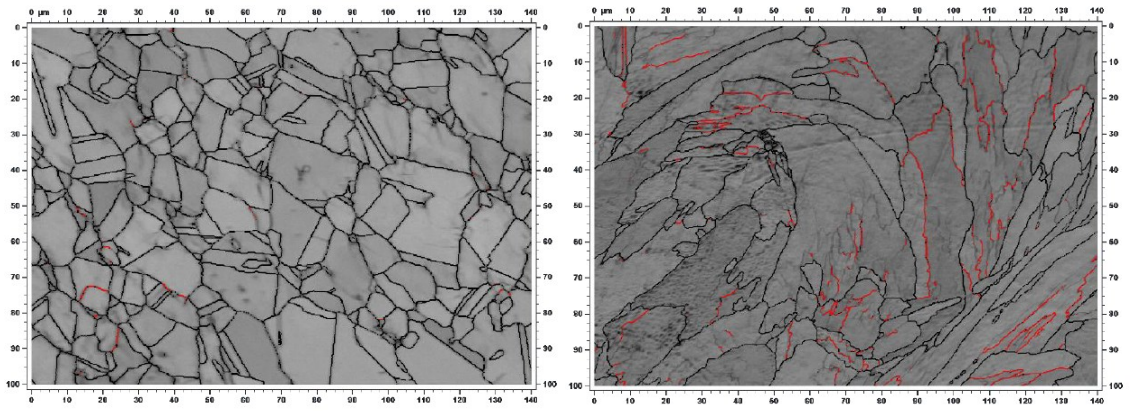

a) b)

Fig. 8: Analyses of grain boundaries for both variants of SS316L: a) cast structure b) powder structure

Conclusion

More extensive study has been done for conventional and 3D printed SS316L as follow up to preliminary ratcheting investigation [13]. Cyclic hardening and subsequent cyclic softening were observed for high loading levels. The square strain path has the strongest influence on additional hardening on the same level of loading. Lower additional hardening due to non-proportional loading has been observed even for circle strain path, i.e. in the 90 degree out of phase test. Cyclic hardening/softening behaviour of conventionally produced specimens differs to 3D printed ones significantly, but the stress-strain behaviour in the half of lifetimes is very similar as visible in Fig. 4b. Fatigue resistance is also comparable for both production technologies considering strain-controlled testing. An accelerated technique based on DIC method application for cyclic stress-strain curve estimation was shown to be comparable with the classical cyclic stress-strain curve. This study has been also done to prepare data for finite element modelling in the area of cyclic plasticity.

Acknowledgement: This research was funded by the Czech Science Foundation (GACR), grant No. 19-03282S, by The Technology Agency of the Czech Republic in the frame of the project TN01000024 and has been done in connection with the DMS project reg. no. CZ.02.1.01/0.0/17_049/0008407 financed by Structural Funds of Europe Union.

References

[1] S. Chen, Z. H. Aitken, Z. Wu, Z. Yu, R. Banerjee, Y-W. Zhang, Hall-Petch and inverse Hall-Petch relations in high-entropy CoNiFeAlxCu1-x alloys. Materials Science and Engineering: A, 773 (2020) 138873.

[2] L. Kunčická, R. Kocich, J. Drápala, V. A. Andreyachshenko, FEM simulations and comparison of the ecap and ECAP-PBP influence on Ti6Al4V alloy's deformation behaviour. In: Proceedings of METAL 2013 - 22nd International Conference on Metallurgy and Materials, 15-17 May 2013, Brno, Czech Republic (2013) 391–396.

[3] R. Kocich, L. Kunčická, A. Macháčková, Twist Channel Multi-Angular Pressing (TCMAP) as a method for increasing the efficiency of SPD. IOP Conf. Ser. Mater. Sci. Eng. 63 (2014) 012006. https://doi.org/10.1088/1757-899X/63/1/012006.

[4] R. Kocich, L. Kunčická, P. Král, A. Macháčková, Sub-structure and mechanical properties of twist channel angular pressed aluminium. Materials Characterization 119 (2016) 75–83. doi:10.1016/j.matchar.2016.07.020.

[5] L. Kunčická, R. Kocich, V. Ryukhtin, J. C. T. Cullen, N. P. Lavery, Study of structure of naturally aged aluminium after twist channel angular pressing, Materials Characterization 152 (2019) 94–100. doi: 10.1016/j.matchar.2019.03.045.

[6] P. C. Angelo, R. Subramanian, Powder metallurgy: Science, technology and applications, 2nd ed., PHI Learning Private Limited, New Delhi, 2008.

[7] R. Zhao, J. Gao, H. Liao, N. Fenineche, C. Coddet, Selective laser melting of elemental powder blends for fabrication of homogeneous bulk material of near-eutectic Ni–Sn composition, Additive Manufacturing 34 (2020) 101261

[8] M. P. Behera, T. Dougherty, S. Singamneni, K. De Silva, Selective laser melting of aluminium metal-matrix composites and the challenges. Materials Today: Proceedings In press, 2020.

[9] S. Pal, N. Gubeljak, R. Hudák, G. Lojen, V. Rajťúková, T. Brajlih, I. Drstvenšek, Evolution of the metallurgical properties of Ti-6Al-4V, produced with different laser processing parameters, at constant energy density in selective laser melting. Results in Physics 17 (2020) 103186

[10] J. J. Marattukalam, V. Pacheco, D. Karlsson, L. Riekehr, J. Lindwall, F. Forsberg U. Jansson, M. Sahlberg, B. Hjörvarsson, Development of process parameters for selective laser melting of a Zr-based bulk metallic glass. Additive Manufacturing 33 (2020) 101124.

[11] N. Li, S. Wu, D. Ouyang, J. Zhang, L. Liu, Fe-based metallic glass reinforced FeCoCrNiMn high entropy alloy through selective laser melting. Journal of Alloys and Compounds 822 (2020) 153695.

[12] J. Ghorbani, J. Li, A. K. Srivastava, Application of optimized laser surface re-melting process on selective laser melted 316L stainless steel inclined parts. Journal of Manufacturing Processes 56(A) (2020) 726-734.

[13] R. Halama, M. Pagáč, Z. Paška, P. Pavlíček, X. Chen, Ratcheting Behaviour of 3D Printed and Conventionally Produced SS316L Material. In: Proceedings of the ASME 2019 Pressure Vessels & Piping Conference PVP2019, July 14-19, 2019, San Antonio, TX, USA, paper number PVP2019- 93384.

[14] J. Hajnyš, M. Pagáč, J. Měsíček, J. Petrů, M. Krol, Influence of scanning strategies parameters on residual stress in SLM process according to bridge curvature method for stainless steel AISI 316L. Materials 13 (2020) 1527. doi: 10.3390/ma13071659.

[15] J. Hajnyš, M. Pagáč, O. Kotera, J. Petrů, S. Scholz, Influence of Basic Process Parameters on Mechanical and Internal Properties of 316L Steel in SLM Process for Renishaw AM400. MM Science Journal, 2019. Pgs: 2790-2794. DOI: 10.17973/MMSJ.2019_03_2018127

[16] L. Hitzler, J. Hirsch, B. Heine, M. Merkel, W. Hall, A. Öchsner, On the anisotropic mechanical properties of selective laser-melted stainless steel. Materials 10 (2017), 1136. DOI: 10.3390/ma10101136

[17] B. Blinn, F. Krebs, M. Ley, C. Gläßner, M. Smaga, J. C. Aurich, R. Teutsch, T. Beck, Influence of the Chemical Composition of the Used Powder on the Fatigue Behavior of Additively Manufactured Materials. Metals 9 (2019), 1285. DOI: 10.3390/met9121285

[18] D. Agius, K. I. Kourousis, C. Wallbrink, A Review of the As-Built SLM Ti-6Al-4V Mechanical Properties towards Achieving Fatigue Resistant Designs. Metals 8 (2018) 75. DOI: 10.3390/ma10101136

[19] M. Sapieta, A. Sapietova, V. Dekys, Comparison of the Thermoelastic Phenomenon Expressions in Stainless Steels During Cyclic Loading. Metalurgija 56 (2017) 203-206. ISSN 0543-5846

[20] P. Kubik, F. Šebek, J. Petruška, J. Hulka, N. Park, H. Huh, Comparative Investigation of Ductile Fracture with 316L Austenitic Stainless Steel in Small Punch Tests: Experiments and Simulations. Theoretical and applied fracture mechanics 98 (2018) 186-198. DOI: 10.1016/j.tafmec.2018.10.005

[21] M. Fusek, D. Ličková, R. Halama, Z. Poruba, F. Fojtík, Evaluation of multiaxial fatigue criteria on LCF data of SS316L. In: Proceedings of Experimental Stress Analysis 2018, Czech Republic: Czech Society for Mechanics, 2018, p. 108-113.

[22] M. Fusek, R. Halama, D. Ličková, Two modification of Jiang criterion for constant amplitude loading of AA2124-T851 AND SS316L. Special issue "Computational Mechanics of Materials" of the Continuum Mechanics and Thermodynamics journal, submitted in 2020.

[23] M. Borodii, S. Shukaev, Additional cyclic strain hardening and its relation to material structure, mechanical characteristics, and lifetime. International Journal of Fatigue 29 (2007) 1184-1191.

[24] R. Halama, P. Gál, Z. Paška, J. Sedlák, A new accelerated technique for validation of cyclic plasticity models. In: Proceedings of MMS 2017 - 22nd Conference on Machine Modeling and Simulation 2017, Sklené Teplice, Slovakia, September 5 – 8 September 2017, Vol. 157, p. 05008. DOI 10.1051/matecconf/201815705008

[25] B. Govindaraj, Digital Image Correlation and its Application for Accelerated Testing of Specimens Manufactured by 3D Printing. Ostrava: VSB - Technical University of Ostrava, Faculty of Mechanical Engineering, Department of Applied Mechanics, 2020, 68 p. Supervisor: prof. Ing. Radim Halama, Ph.D.